Electronic Supplementary Information for

Impact of Sequential Surface-Modification of Graphene Oxide on Ice Nucleation

Caroline I. Biggs[a], Christopher Packer,[a] Marc Walker,[c] Jonathan P. Rourke[a] and Matthew I. Gibson[a,b]*

a Department of Chemistry, University of Warwick, Coventry, CV4 7AL, UK.

b Warwick Medical School, University of Warwick, Coventry, CV4 7AL, UK

c. Department of Physics, University of Warwick, Coventry, CV4 7AL, UK

Corresponding Author Contact Details

Professor Matthew I. Gibson. m.i.gibson@warwick.ac.uk

Experimental Section

Materials

4,4'-azobis(4-cyanovaleric acid) (98%), *N*-isopropyl acrylamide (98%), potassium phosphate tribasic, 2-bromo-2-methylpropionic acid, carbon disulphide, methylamine (98%), glacial ethanoic acid L-cysteine (98%), 1-dodecanethiol (98%), 1-hexanethiol (95%) and 1-octadecanethiol (98%) were purchased from Sigma-Aldrich. Hexane, methanol, acetone, dichloromethane, toluene, diethyl ether, acetonitrile and tetrahydrofuran were purchased from Fluka.

Analytical and physical methods

^{1}H and ^{13}C NMR spectra were recorded on Bruker DPX-300 and DPX-400 spectrometers using deuterated solvents purchased from Sigma-Aldrich. Chemical shifts are reported relative to residual non-deuterated solvent. Size exclusion chromatography (SEC) was used to examine and differentiate between the molecular weights and dispersities of the synthesized polymers. The SEC analysis was performed on a Varian 390-LC MDS system equipped with a PL-AS RT/MT autosampler, a PL-gel 3 μm (50 × 7.5 mm) guard column, two PL-gel 5 μm (300 × 7.5 mm) mixed-D columns held at 30 °C and the instrument equipped with a differential refractive index and a Shimadzu SPD-M20A diode array detector. Dimethylformamide (including 5 mM ammonium tetrafluoroborate) was used as the eluent at a flow rate of 1 mL min^{-1}. Transmission FT-IR (Fourier Transform-Infrared Spectroscopy) spectra were recorded, using a Bruker ALPHA FT-IR spectrometer, for each sample with an acquisition time of 1 hour. TGA was performed on each sample of grafted bwGO using a Mettler-Toledo TGA/DSC1 under a nitrogen atmosphere between 30-1000 °C. Scanning Electron Microscopy: The samples were sonicated in vials of DI water before drop casting onto silicon wafer. A Zeiss Gemini FEGSEM

was utilised for the imaging, set to 0.5keV and imaged by In-Lens detector, with a WD of ~1.8mm.

Ice nucleation assay

The temperature of the ice and water droplets was controlled on a Linkam Biological Cryostage BCS196 with T95-Linkpad system controller equipped with a LNP95-Liquid nitrogen cooling pump, using liquid nitrogen as the coolant (Linkam Scientific Instruments UK, Surrey, UK). Images and droplet monitoring was conducted using a Veho Discovery VMS-004 Deluxe USB microscope and Veho Microcapture software V 1.3.

The assay described is for one sample of grafted bwGO; the method was repeated for each sample of functionalised bwGO. A known mass of the grafted bwGO was suspended in Milli Q water with the solution then subjected to sonication (20 minutes) to increase the dispersity and accuracy of concentration of the sample in water. A concentration of 2.5 $mg.mL^{-1}$ was used, unless specified otherwise. 8 or 9 droplets (1 µL) were pipetted onto a glass slide covered with a hydrophobic barrier, ensuring that the droplets are clearly separated. The slide was placed inside a Linkham Scientific cryostage where it was cooled to -40 °C from 15 °C at a rate of 2 °C/minute, which allows for equilibrium before freezing temperatures are reached. Cooling is achieved using a Linkam-LNP95 cooling pump which flows a precisely controlled stream of liquid nitrogen into the sample chamber. The Ice nucleation process was observed through a Veho Discovery VMS-004 Deluxe USB microscope and Veho Microcapture software V 1.3. The experiment was repeated (at least) twice more using new droplets from the stock solution, recording a minimum of 24 freezing temperatures for each sample.

Synthetic Procedures

Graphene Oxide

The bwGO material used in this study was prepared via the Hummers synthesis and a NaOH wash, as described elsewhere.[1,2]

Hummers Synthesis of GO

Natural flake graphite (5.020 g) and KNO_3 (4.507 g) were suspended, with stirring, in concentrated sulphuric acid (169 ml). The mixture was cooled on ice and $KMnO_4$ (22.443 g) was added over 70 minutes. The mixture was then allowed to warm to room temperature with constant stirring. After 24 hours the green solution had become too thick to stir. It was left for a further 4 days over which time there was a colour change to purple. This mixture was slowly dispersed into 550 ml 5 wt% H_2SO_4 in water over the course of one hour and left to stir for a further 3 hours. Hydrogen peroxide (45ml, 30 vol, equivalent to 15g) was then added to the brown mixture over 5 minutes, with considerable effervescence, leaving a glittery gold suspension which was left stirring for 2 hours. This suspension was then further diluted with 500 ml of 3 wt% H_2SO_4/0.5 wt% H_2O_2 in H_2O and left stirring for 12 hours. The mixture was centrifuged (12,500 rpm (18,200 X g), 20 min) and the separated solid was collected, re-dispersed into 500 ml of 3 wt% H_2SO_4/0.5 wt% H_2O_2 in H_2O and re-centrifuged. In total, 6 such acidic washes were done, followed by 8 washes with pure water giving a neutral pH. After 3 washes the glittery flakes had all disappeared leaving a much thicker, darker mixture. The resultant brown solution was dried under vacuum to give a brown film-like solid (5.0955 g).

EDX atomic % (standard deviation): C 58 (1); O 40 (2).

NaOH wash of GO to give bwGO

Hummers GO. 140 mg of Hummers GO was re-dispersed into H_2O (250 ml) by mild sonication to form a stable light brown solution. NaOH was added (0.140 g), under constant stirring, to give a 0.014 M solution. There was immediate darkening on dissolution of the NaOH. The solution was then heated to 70 °C for 1 hour. The resultant dark brown solution was centrifuged (12,500 rpm, (18,200 X g), 30 minutes) leaving a dark brown solid and colourless supernatant. This supernatant, and that of all subsequent centrifuge cycles, was collected. The dark brown solid was washed with water and re-centrifuged. The solid was re-protonated with dilute HCl (250 ml, 0.014 M) and stirred for 1 hour at 70 °C. Once cool, the solid was collected as before and washed with water. The wet solid could then be dried under vacuum to give to a black solid (90.3 mg, 65%) or dispersed in a H_2O/CH_3CN mixture via sonication.

The collective supernatants were dried under vacuum to give an off-white powder (239.1 mg) of OD contaminated with NaCl (calculated to be 204.5 mg), i.e. 34.6 mg (25%) of OD.

EDX atomic % (standard deviation): C 76 (1); O 21 (1); Na 1.9 (0.4); Cl 1.0 (0.1).

Synthesis of 2-(dodecylthiocarbonothioylthio)-2-methylpropanoic acid (RAFT agent)

The 2-(dodecylthiocarbonothioylthio)-2-methylpropanoic acid (DMP) RAFT agent was synthesised following the literature method.[3] To a stirred suspension of K_3PO_4 (4.20g, 19.76 mmol) in acetone (60 mL) was added dodecanethiol (4.00 g, 19.76 mmol) dropwise over 25 minutes. CS_2 (4.10 g, 53.85 mmol) was added and stirred for 10 minutes; the solution turned bright yellow. 2-bromo-2-methylpropionic acid (3.00 g, 17.96 mmol) was added; a precipitation of KBr was noted. The reaction was stirred for 18 hours and then the solvent was removed under reduced pressure and the residue was extracted into CH_2Cl_2 (2 x 200 mL) from 1M HCl (200 mL). The organic layer was washed with water (200 mL) and brine (200 mL) then dried over $MgSO_4$. The solvent was removed under reduced pressure to yield the crude

product. Purification was carried out by column chromatography on silica (eluting with 75:24:1 40 – 60 °C petroleum ether: diethyl ether: acetic acid) to yield a bright yellow solid (4.20 g, 64 %).

^{1}H NMR (300 MHz, $CDCl_3$) δ_{ppm}: 3.20 (2H, t, S-C**H**$_2$-$(CH_2)_{10}$- CH_3); 1.66 (6H, s, C-(C**H**$_3$)$_2$); 1.60 (2H, p, S-CH_2-C**H**$_2$-$(CH_2)_9$-CH_3); 1.31 (2H, m, S-CH_2-CH_2-C**H**$_2$-$(CH_2)_8$-CH_3); 1.25-1.15 (16H, m, S-CH_2-CH_2-CH_2-(C**H**$_2$)$_8$-CH_3); 0.82 (3H, t S-CH_2-$(CH_2)_{10}$- C**H**$_3$).

Polymerisation of *N*-isopropylacrylamide (NIPAM)

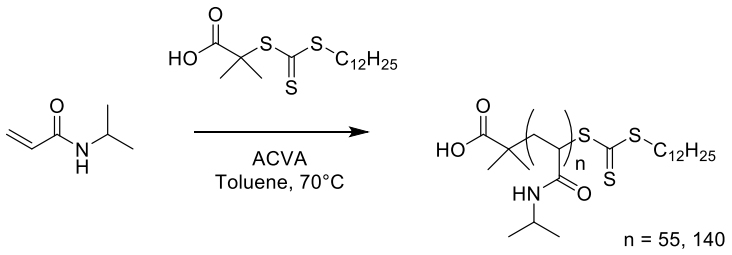

Scheme S1. Synthetic route for the polymerisation of NIPAM.

Prepared according to a method adapted from literature.[3] In an example procedure, *N*-isopropyl acrylamide (1.00 g, 8.84 mmol), 2-(dodecylthiocarbonothioylthio)-2-methylpropanoic acid (32.22 mg, 88.4 μmol), and 4,4'-azobis(4-cyanovaleric acid) (ACVA) (4.95 mg, 17.7 μmol) were all dissolved in methanol/toluene (1:1; 4 mL). The solution was then degassed by bubbling with nitrogen gas for 30 minutes and subsequently heated in an oil (70 °C, 35 min). The solution was concentrated and then precipitated into diethyl ether (45 mL), re-precipitated and purified from THF into diethyl ether (45 mL). The product can then be purified 3 times by precipitation from toluene into diethyl ether, isolated centrifugation, and dried under vacuum overnight with a resultant yellow solid.

pNIPAM$_{55}$: Conversion (NMR): 85%, M_n (SEC): 6200 gmol^{-1}, Dispersity (SEC): 1.08. **^{1}H NMR** ($CDCl_3$) δ_{ppm}: 3.90-4.10 (1H, br, H^a); 2.00-2.30 (2H, br, H^b); 1.45-1.90 (1H, br, H^c); 1.00-1.40 (6H, m, H^d).

pNIPAM$_{140}$: Conversion (NMR): 60.5%, M_n (SEC): 15700 gmol^{-1}, Dispersity (SEC): 1.11. **^{1}H NMR** ($CDCl_3$) δ_{ppm}: 3.90-4.15 (1H, br, H^a); 1.90-2.30 (2H, br, H^b); 1.50-1.70 (1H, br, H^c); 1.0-1.50 (6H, m, H^d).

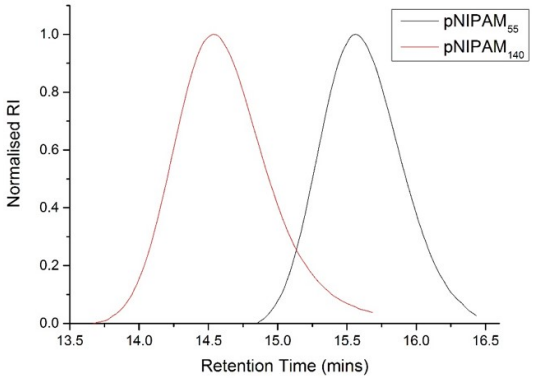

Figure S1. SEC analysis of the RAFT mediated pNIPAM polymers

Table S1. Summary of polymer analysis from SEC and NMR.

	Polymer	DP [a]	Conversion (%) [b]	Mn (SEC)	Mw (SEC)	Dispersity
1	pNIPAM	140	60.5	15700	17400	1.11
2	pNIPAM	55	85.0	6200	6700	1.08

[a] calculated from SEC data. [b] determined from NMR using mesitylene as a reference.

Grafting of thiols to the surface of graphene oxide

Grafting to the surface of bwGO can be achieved using standard Schlenk conditions under a nitrogen atmosphere. Methylamine (3 mL) was added to a solution of pNIPAM (20 mg) in DMF (3 mL) together with a catalytic amount of glacial ethanoic acid, generating effervescence. The mixture was then immediately transferred into a solution of bwGO (60 mg) in DMF (120 mL). The mixture of bwGO/pNIPAM was then heated to 50 °C for 1 hour, before being allowed to cool to room temperature and left to stir under nitrogen gas overnight (16 hours). The product was collected via centrifugation (13,200 rpm (20,200 X g) for 20 minutes), and was washed with water (30 minutes x 5) before being dried on a freeze dryer/under vacuum to remove excess water and leave a black solid. The polymer sample was interchanged in the method with a range of thiols, using the same quantities as stated, to vary the grafted molecule.

Additional Data

Thermogravimetric Analysis (TGA)

It has been suggested that nanocomposites materials show a major decomposition at a higher temperature than both bwGO and the isolated polymer or thiol.[4] This is thought to be due to the decomposition of the functional groups on the basal plane, edge, and vacancies in the structure, but this still needs clarification.[5] The stability, with regards to the epoxy groups on the surface, is vague due to the random surface distribution,[6] so it cannot be conclusive as to whether a grafted polymer, or thiol, will indeed increase the thermal stability of the bwGO sheet. As a result, any deviation from the decomposition profile of bwGO observed in the profile of the functionalised bwGO (Figure S2), may show a form of modification.

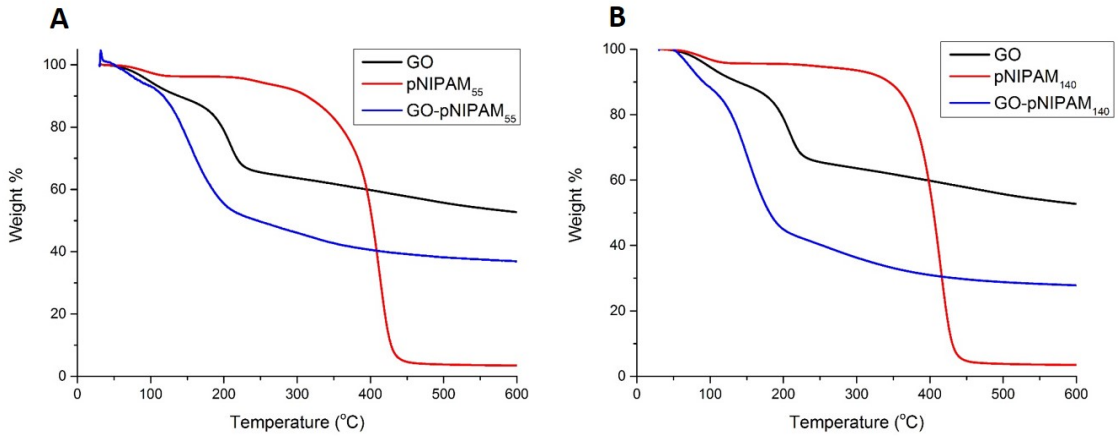

Figure S2. [A] Decomposition profile of $pNIPAM_{55}$ grafted to bwGO and its isolated components; [B] Decomposition profile of $pNIPAM_{140}$ grafted to bwGO and its isolated components.

The profiles of bwGO functionalised with the two pNIPAM samples (Figure S2), show a distinct change from that of bwGO. Supported by another obvious variation with the decomposition of the isolated polymer, it can be determined that the bwGO sheet has been modified in some form, and it is therefore likely that the polymer has been grafted to the surface. It may be expected that a large mass loss would be present around 400 °C due to the decomposition temperature of the NIPAM monomer, which is not the case for the bwGO-pNIPAM profiles. The fact that the mass loss is not observed, exposes changes to the stability of both bwGO and the polymer, with the potential for the thermal stability of the polymer being increased by anchoring to the carbon surface, leading to an expected mass loss beyond the 600 °C that has been measured. Similar evidence can be found with the comparison of the thiol grafted samples to the same bwGO profile (Figure S3). It should be note that the grafting density is very low for all of the composites, as confirmed by TGA and IR spectroscopy, making their dramatic nucleation altering properties even more remarkable.

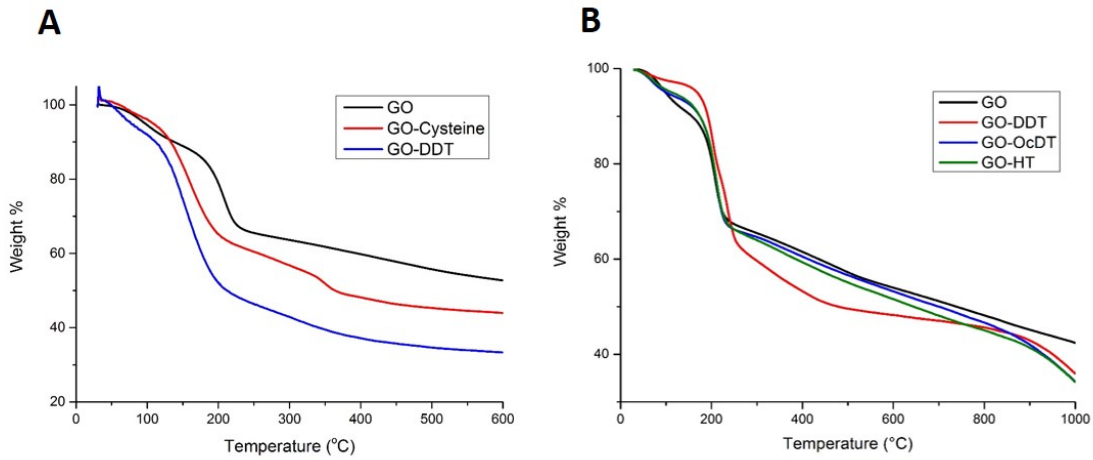

Figure S3. TGA data showing the trend in thermal decomposition of bwGO when cysteine dodecanethiol, hexanethiol and octadecanethiol are grafted to the surface.

Infrared Spectroscopy

Long acquisition IR (acquisition times of 1 hour) was required to provide spectra with well-defined peaks. Should the 'grafting to' method have been successful, the most obvious transformation in the spectra will be an increase in intensity of the broad –OH peak between 2500 cm^{-1} and 3700 cm^{-1} as a result of epoxide ring opening, adding to the stretch present from the alcohol and carboxylic acid groups decorated the edges of bwGO. Alterations in the –CH regions at 2850-3000 cm^{-1} and 1350-1480 cm^{-1} will be indicative of the presence of the alkane chain found in each of the hydrophobic thiols. However, these peaks may be difficult to distinguish depending on the length of alkane chain and grafting density; ultimately the number of –CH moieties present. Besides the –OH peak change, the bwGO samples grafted with pNIPAM can be expected to show peaks transmitted at 1653, 1554 and 1381 cm^{-1} that are assigned to the C=O of the amide.[7] As seen in Figure S4, the bwGO-DDT sample clearly displays each of the aforementioned alterations to the IR spectra expected of a functionalised bwGO sheet. An increase in intensity for the –OH peaks, sharp peaks around 2850-3000 cm^{-1}

representing the alkane CH's, and finally, an obvious change to the –CH region lower down the scale (1000-2000 cm^{-1}).

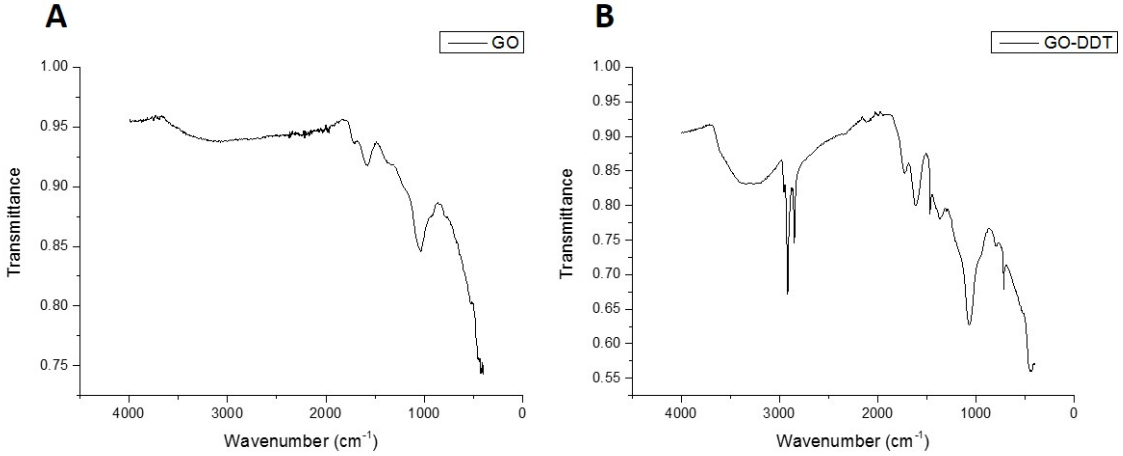

Figure S4. IR spectra of [A] Isolated bwGO sheets; [B] bwGO functionalised with dodecanethiol using– an example of the expected changes to the bwGO spectra with alkane thiols grafted to the surface.

IR spectra obtained for the grafting of pNIPAM to bwGO also showed the expected changes. Between 1500 and 1750 cm^{-1}, a new peak can be seen when compared to the spectra of bwGO, as is the case for the presence of an amide carbonyl. The discussed changes in –OH peak and –CH peaks are also noted in the spectra for bwGO-pNIPAM$_{55}$, and the other alkane thiols (Figure S5).

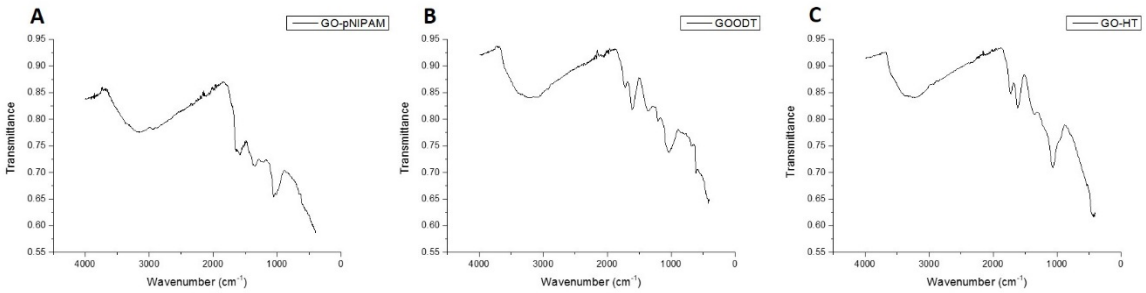

Figure S5. IR spectra for [A] pNIPAM, [B] octadecanthiol and [C] hexanethiol grafted to bwGO

X-ray Photoelectron Spectroscopy (XPS)

XPS spectroscopy was used to confirm the successful functionalisation of the bwGO with the small molecules thiols and polymers. It should be notes that it is not possible to observe any of the C-S bonds due to them being present in the same region as the C-C bonds. The expected graphene energy loss features due to π to π^* transitions (shake-up) are visible in all of the samples. In Figure S7, the C=O-N bonds are observed in the bwGO-pNIPAM samples only, corresponding to the expected structure for the grafted polymers.

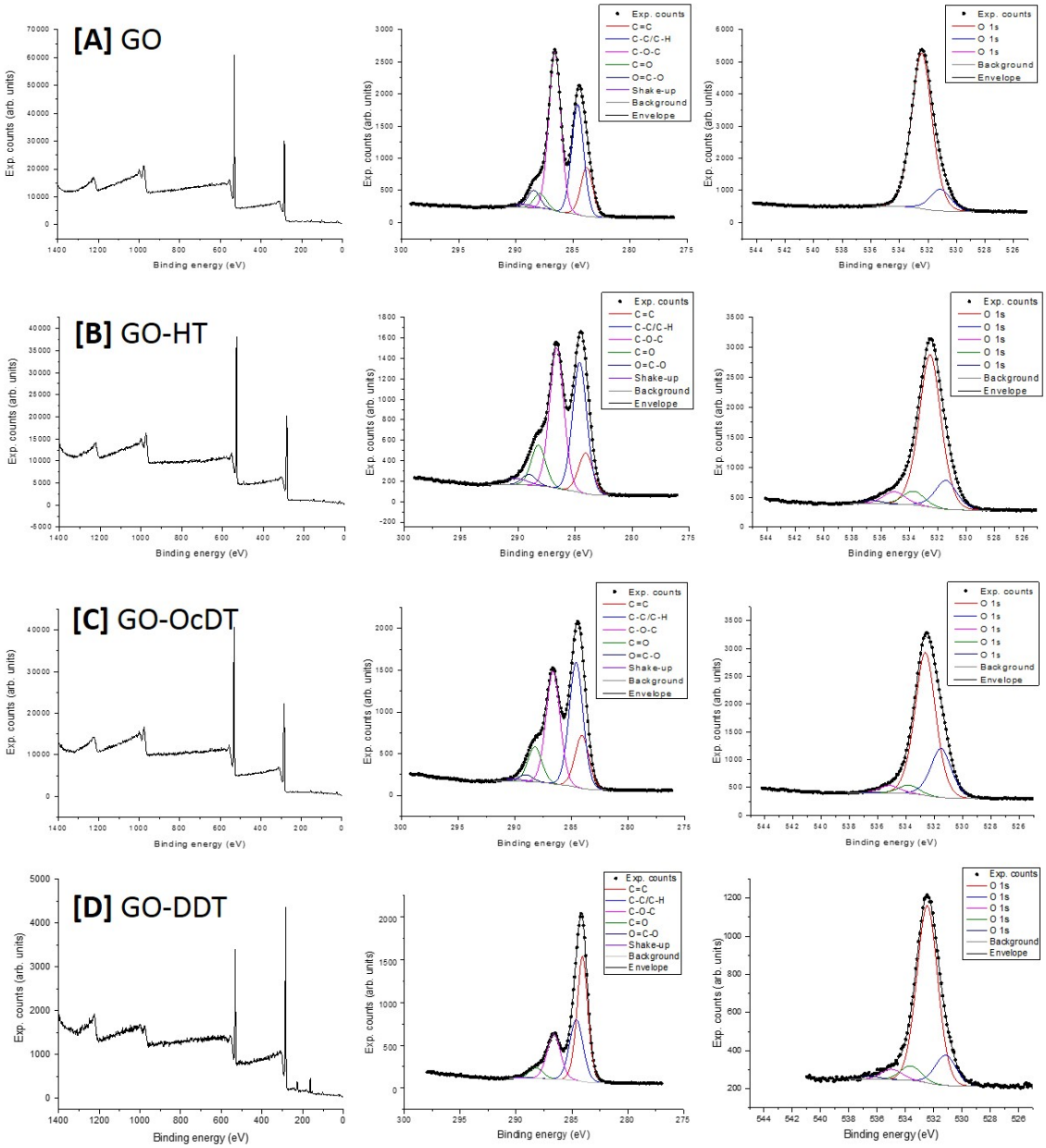

Figure S6. XPS survey scans and fitted spectra for bwGO, bwGO-hexanethiol, bwGO-Octadecanethiol and bwGO-dodecanethiol

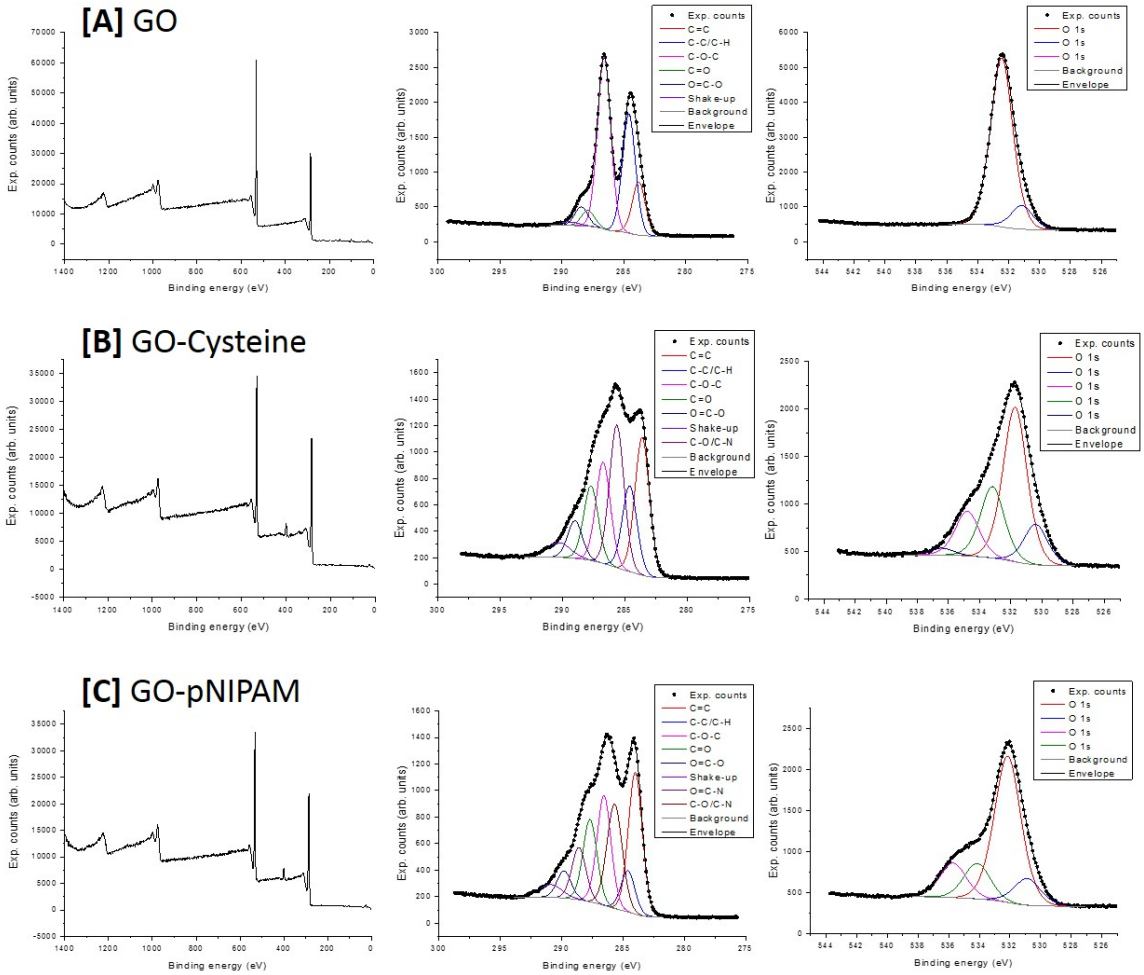

Figure S7. XPS survey scans and fitted spectra for bwGO, bwGO-cysteine and bwGO-pNIPAM

Scanning Electron Microscopy (SEM) of GO's

To study the aggregation state and morphology of the GO's SEM was employed, Figure S8. In all cases a wide distribution of GO sheet sizes was observed, as would be expected for heterogeneous materials such as this. There was some evidence of aggregated sheets but it was not clear if any particular surface coating lead to more aggregation than another.

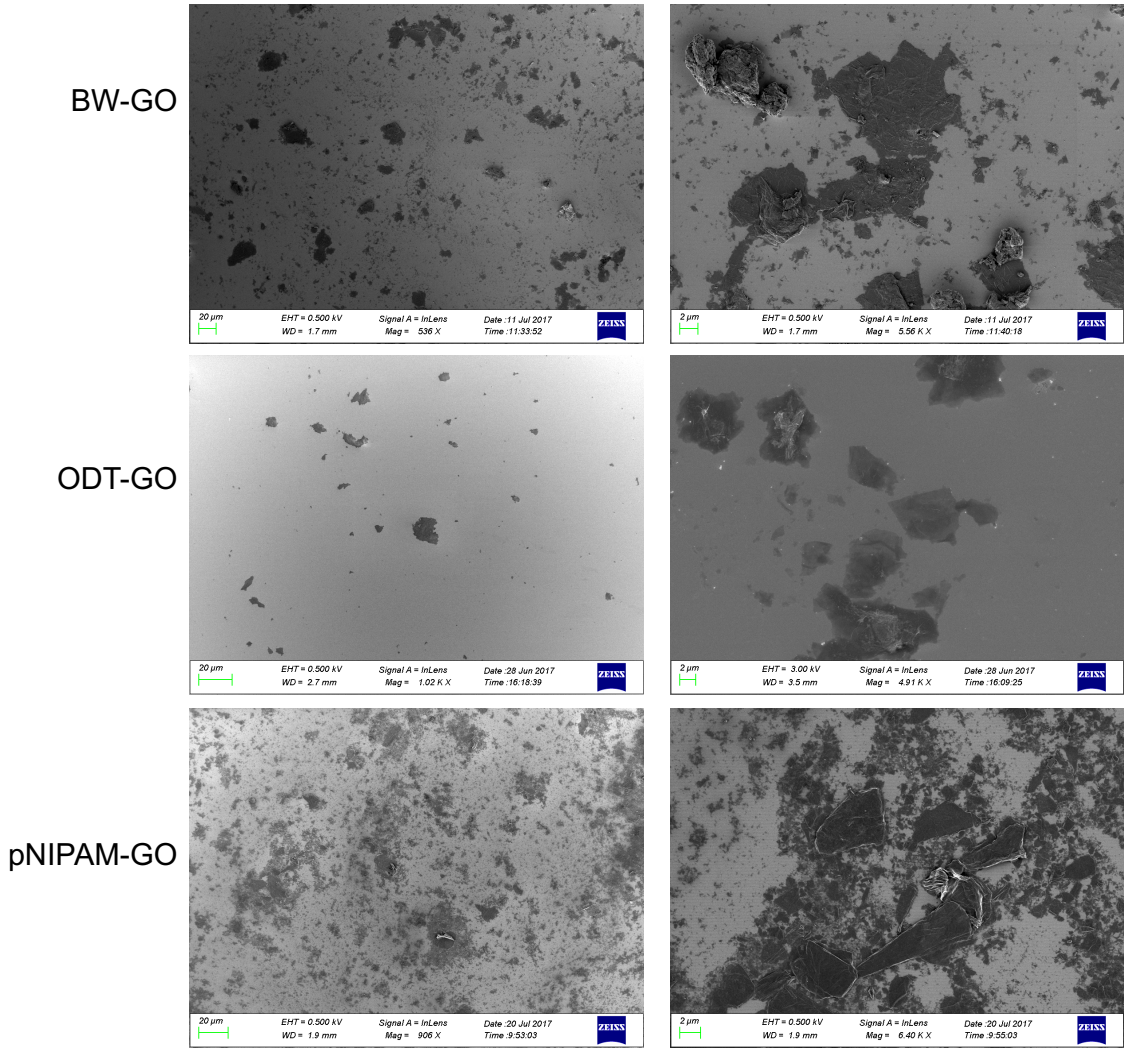

Figure S8. Scanning electron microscope images of the GO's with and without modifications

Additional Nucleation Data

As an alternative to the INI spectra presented in the main paper, box and whisker plots (Figure S8) can be used to directly compare the INI activity of each of the nuclei. The representation evidently shows the hydrophobic thiol modified bwGO promote nucleation and the polymer modified bwGO also promote nucleation, but to a much lesser extent. It should be noted that the whiskers on the plots represent the standard deviation of the recorded nucleation temperatures, as this is more important than the upper and lower boundaries when considering the stochastic nature of water freezing. The box indicates the 25-75 percentiles, and the median (centre line).

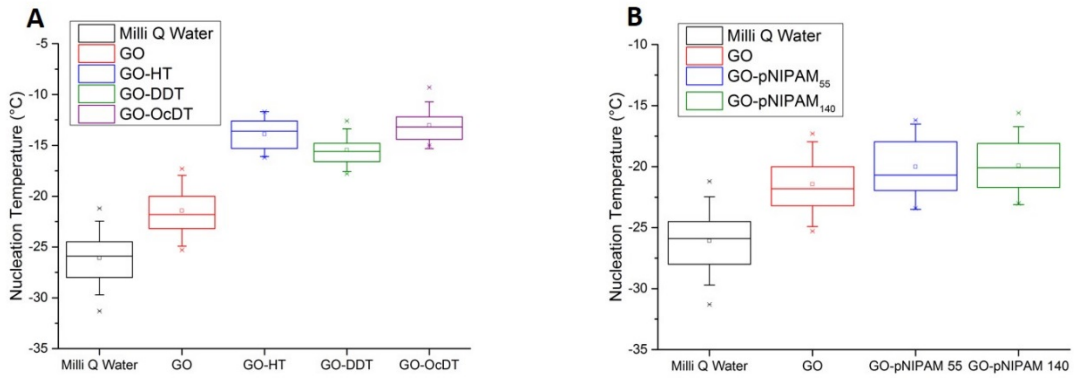

Figure S9. Ice nucleation distribution comparing any differences when the alkane thiol anchored to bwGO's surface is changed, using [A] hexanethiol, dodecanethiol, and octadecanethiol; [B] pNIPAM

In order to investigate how the total surface area of nucleating species can change the nucleation temperature, it was planned to carry out INI experiments at higher concentrations. Unfortunately, at concentrations above 2.5 $mg.mL^{-1}$ the sample droplets were unstable and could not be measured. Instead, lower concentrations were investigated, using the most potent nucleator: bwGO-octadecanthiol. As can be seen in Figure S10, as would be expected, the

greater the number of nucleating species present in the sample (higher concentration) the greater the chance of catalysing the freezing of the droplet. Despite this, the bwGO-OcDT nuclei are still potent promoters even at 0.1 mg/mL in a 1 µL droplet. Even though the bwGO-OcDT nuclei is not as potent at lower concentrations, it is still a vast improvement on the nucleating ability of bwGO and is one of the best nuclei reported to date.

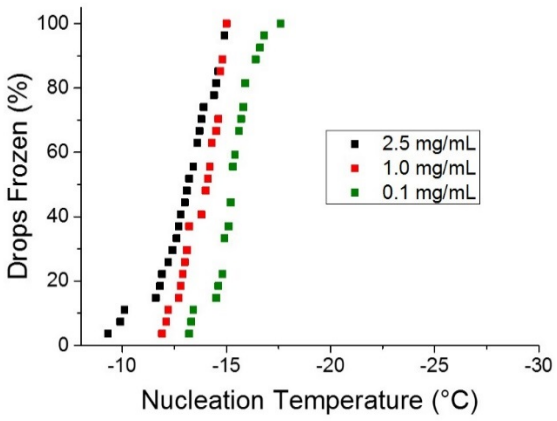

Figure S10. Concentration dependent ice nucleation distributions of bwGO-OcDT at 2.5, 1.0, and 0.1 mg.mL

References

(1) Thomas, H. R.; Day, S. P.; Woodruff, W. E.; Valles, C.; Young, R. J.; Kinloch, I. A.; Morley, G. W.; Hanna, J. V.; Wilson, N. R.; Rourke, J. P. *Chem. Mater.* **2013**, *25* (18), 3580–3588.

(2) Rourke, J. P.; Pandey, P. A.; Moore, J. J.; Bates, M.; Kinloch, I. A.; Young, R. J.; Wilson, N. R. *Angew. Chemie Int. Ed.* **2011**, *50* (14), 3173–3177.

(3) Phillips, D. J.; Gibson, M. I. *Biomacromolecules* **2012**, *13* (10), 3200–3208.

(4) Thomas, H. R.; Phillips, D. J.; Wilson, N. R.; Gibson, M. I.; Rourke, J. P. *Polym. Chem.* **2015**, *6* (48), 8270–8274.

(5) Larciprete, R.; Fabris, S.; Sun, T.; Lacovig, P.; Baraldi, A.; Lizzit, S. *J. Am. Chem. Soc.* **2011**, *133* (43), 17315–17321.

(6) Larciprete, R.; Lacovig, P.; Gardonio, S.; Baraldi, A.; Lizzit, S. *J. Phys. Chem. C* **2012**, *116* (18), 9900–9908.

(7) Shi, S.; Zhang, L.; Wang, T.; Wang, Q.; Gao, Y.; Wang, N. *Soft Matter* **2013**, *9* (46), 10966.